13. N. Brustovetsky and M. Klingenberg, *Biochemistry* **35**, 8483 (1996).
14. I. Marzo *et al.*, *Science* **281**, 2027 (1998).
15. G. Stepien, A. Torroni, A. B. Chung, J. A. Hodge, D. C. Wallace, *J. Biol. Chem.* **267**, 14592 (1992).
16. A. Doerner *et al.*, *FEBS Lett.* **414**, 258 (1997).
17. To amplify the coding region of human *ANT1* (GenBank accession number, J04982), we designed primers from intronic sequences flanking the following exons: exon 1, 1F (5′-GCTCGGCGGGACAGATAACATGAAT) and 1R (5′-TGCGCATAAGACGGTGCCAAAAATA); exon 2, 2F (5′-AATCTAGGAAGTGCAAACC) and 2R (5′-TGTGAGTTATAGATCCCATA); exon 3, 3F (5′-GCAAGGTCAGAGCATGGA) and 3R (5′-TGTAAAATGTTCTCCTCGG); exon 4, 4F (5′-ATGCCCAGATGACCCTGATT) and 4R (5′-AACCACACAATGGATCTGTG). Polymerase chain reaction (PCR) amplification was carried out in a volume of 50 μl containing 50 ng of genomic DNA, 0.2 μM of each primer plus 200 μM of each dNTP, and 1.25 U of DNA polymerase (Dynazyme, Finnzymes, Finland). Cycling conditions were as follows: 95°C for 30 s, 56°C for 30 s, and 72°C for 45 s; 33 cycles, with an initial 3-min denaturation at 95°C and a final 10-min extension at 72°C. To amplify exon 1, we included 1 M betaine (Sigma). DNA sequence was analyzed by PCR-cycle sequencing and visualized by 377 ABI Sequencer (Applied Biosystems, Foster City, CA).
18. M. Zeviani, data not shown.
19. Haplotype construction and linkage calculations of the chromosome 3 adPEO region marker data with the updated clinical information were done as described (*10*).
20. A. Suomalainen and M. Zeviani, unpublished data.
21. R. Carrozzo, M. M. Davidson, W. F. Walker, M. Hirano, A. F. Miranda, *J. Neurol. Sci.* **170**, 24 (1999).
22. M. K. A. Bauer, A. Schubert, O. Rocks, S. Grimm, *J. Cell Biol.* **147**, 1493 (1999).
23. Yeast cells were grown at 30°C in YPD (1% yeast extract, 2% peptone, 2% glucose) or in synthetic complete medium, with 2% glucose (SCD) or 2% glycerol (SCG) as the carbon source, respectively. Yeast transformants were selected on SCD-Ura and tested for growth on SCG-Ura (*36*). The single-copy *AAC2* expression vector, pSEYc58AAC2 (*27*), was a *CEN-ARS URA3* plasmid encoding the wild-type AAC2 derived from genomic DNA of *S. cerevisiae* (GenBank accession number J04021). The vector control, pSEYc58, was obtained by removing the *AAC2* fragment from pSEYc58AAC2 by Pvu II digestion. For the mutagenesis, the *AAC2* fragment from pSEYc58AAC2 was released and inserted into pGEM-4Z (Promega) to obtain pGEMAAC2. Mutagenesis was carried out with the Chameleon kit (Stratagene). The mutagenesis primer introduced the analogous Ala→Pro substitution to *AAC2* (amino acid 128), as in human ANT1 (amino acid 114). Screening of the mutant colonies was carried out by PCR and solid-phase minisequencing (*37*). The mutant pGEMAAC2 insert was released and inserted back into pSEYc58 to obtain pSEYc58aac2^{A128P}. The correct orientation and sequence of the insert were confirmed by DNA sequencing.
24. Yeast total genomic DNA was extracted by standard methods and digested with Acc I (New England Biolabs, Herts, UK). The concentration of DNA in the samples was determined spectrophotometrically after the digestion to confirm loading of equal amounts of DNA (3 μg). Southern hybridization analysis was carried out by standard methods, with a 5′-[γ-^{32}P]ATP end-labeled yeast mtDNA-specific sequence repeat (5′-CTCCTTTCGGGGTTCCGGCTCCCGTGG CCGGG CCCCGG-3′) as a hybridization probe.
25. J. E. Walker and M. J. Runswick, *J. Bioenerg. Biomembr.* **25**, 435 (1993).
26. V. Müller, G. Basset, D. R. Nelson, M. Klingenberg, *Biochemistry* **35**, 16132 (1996).
27. D. R. Nelson, J. E. Lawson, M. Klingenberg, M. G. Douglas, *J. Mol. Biol.* **230**, 1159 (1993).
28. All of the proteins used for sequence comparison were retrieved from SWISS-PROT by Entrez query. Version 1.8 of ClustalW at European Bioinformatics Institute (http://www2.ebi.ac.uk/clustalw/) with default parameters was used for multiple sequence alignment, and DNAMAN software (Lynnon Biosoft) for graphical enhancement. The secondary-structure predictions were carried out with the PHDsec program (*38*).
29. H. D. Bakker *et al.*, *J. Inherit. Metab. Dis.* **16**, 548 (1993).
30. B. H. Graham *et al.*, *Nature Genet.* **16**, 226 (1997).
31. L. A. Esposito, S. Melov, A. Panov, B. A. Cottrell, D. C. Wallace, *Proc. Natl. Acad. Sci. U.S.A.* **96**, 4820 (1999).
32. I. Nishino, A. Spinazzola, M. Hirano, *Science* **283**, 689 (1999).
33. J. Bodenstein-Lang, A. Buch, Follmann H. *FEBS Lett.* **258**, 22 (1989).
34. P. Young, J. M. Leeds, M. B. Slabaugh, C. K. Mathews, *Biochem. Biophys. Res. Commun.* **203**, 46 (1994).
35. L. J. Yan, R. S. Sohal, *Proc. Natl. Acad. Sci. U.S.A.* **95**, 12896 (1998).
36. J. Toikkanen *et al.*, *Yeast* **12**, 425 (1996).
37. A.-C. Syvänen, *Clin. Chim. Acta.* **226**, 225 (1994).
38. B. Rost and C. Sander, *Proteins* **19**, 55 (1994).
39. V. Tiranti, data not shown.
40. M. Zeviani *et al.*, *Neurology* **38**, 1339 (1988).
41. A. M. Viola, C. L. Galeotti, P. Goffrini, A. Ficarelli, I. A. Ferrero, *Curr. Genet.* **27**, 229 (1995).
42. T. Drgon, L. Sabova, G. Gavurnikova, J. Kolarov, *FEBS Lett.* **304**, 277 (1992).
43. J. Juselius and S. Keränen, data not shown.
44. We thank T. Fox for pSEYc58AAC2 and advice, D. Nelson for strain DNY1, and A. M.Viola for VG1-5A strain; G. Galassi, M. G. Piscaglia, and F. Salvi for clinical characterization of patients; E. Shoubridge and K. Wartiovaara for helpful discussions; and R. Timonen, P. Tainola, F. Carrara, and A. Bordoni for technical assistance. Supported by grants from the Maud Kuistila Memorial Foundation, Oskar Öflund Foundation, and Finnish Medical Foundation (J.K.); Telethon-Italy (grant 1180), Ministero della Sanita (030.3/RF98.37), and European Union Human Capital and Mobility on "mitochondrial biogenesis in development and disease" (M.Z.); the Academy of Finland grant 42160 (S.K.); the Emil Aaltonen Foundation (A.S.); and Helsinki Graduate School in Biotechnology and Molecular Biology (J.J.).

14 February 2000; accepted 16 June 2000

Involvement of Cellular Caveolae in Bacterial Entry into Mast Cells

Jeoung-Sook Shin, Zhimin Gao, Soman N. Abraham*

Caveolae are subcellular structures implicated in the import and transcytosis of macromolecules and in transmembrane signaling. To date, evidence for the existence of caveolae in hematopoietic cells has been ambiguous. Caveolae were detected in the microvilli and intracellular vesicles of cultured mouse bone marrow–derived mast cells (BMMCs). CD48, a receptor for FimH-expressing (type 1 fimbriated) *Escherichia coli*, was specifically localized to plasmalemmal caveolae in BMMCs. The involvement of caveolae in bacterial entry into BMMCs was indicated because caveolae-disrupting and -usurping agents specifically blocked *E. coli* entry, and markers of caveolae were actively recruited to sites of bacterial entry. The formation of bacteria-encapsulating caveolar chambers in BMMCs represents a distinct mechanism of microbial entry into phagocytes.

Originally defined by their cavelike morphology (*1*), caveolae are pleomorphic membrane structures characterized biochemically by their buoyant density; resistance to nonionic detergents; and enrichment in cholesterol, glycolipids such as the glycosphingolipid G_{M1}, and a specific protein, caveolin (*2–4*). Caveolae participate in the transcytosis of macromolecules across capillary endothelial cells (*5*) and in the concentration of small molecules internalized by potocytosis (*6*). They also serve as conduits for transmembrane signaling, containing high concentrations of signaling molecules (*7*, *8*). Although believed to be present in virtually all cell types, the presence of caveolae in hematopoietic cells has not been clear. Cell lines of lymphocytes (*9*) and mast cells (*10*) appear to possess membrane domains consistent with caveolae but have not been shown to contain caveolin. We investigated whether mouse BMMCs form caveolae. Mast cells play a crucial role in recruiting neutrophils to sites of bacterial infection (*11*, *12*). They can also phagocytose a wide range of bacteria (*13*). In antibody-deficient conditions, however, these cells and other phagocytes support the entry and subsequent survival of FimH-expressing *E. coli* (*14*, *15*).

Caveolar fractions were isolated from BMMCs (Fig. 1A). Immunogold microscopy of cross sections of BMMCs with caveolin-specific antibody labeled microvilli and intracellular vesicles (Fig. 1D). Thus, although BMMCs did not appear to form cavelike caveolae in their plasma membranes, vesicular and plasmalemmal forms of caveolae were present. The presence of glycosylphosphatidylinositol (GPI)-anchored molecules in native caveolae is controversial (*16–18*). We determined that CD48, a GPI-anchored molecule, was associated with caveolae of BMMCs (Fig. 1, A and C). Confocal microscopy of BMMCs revealed colocalization of CD48 with caveolin primarily in the plasma

Departments of Pathology and Microbiology, Duke University Medical Center, Durham, NC 27710, USA.

*To whom correspondence should be addressed. E-mail: abrah006@mc.duke.edu

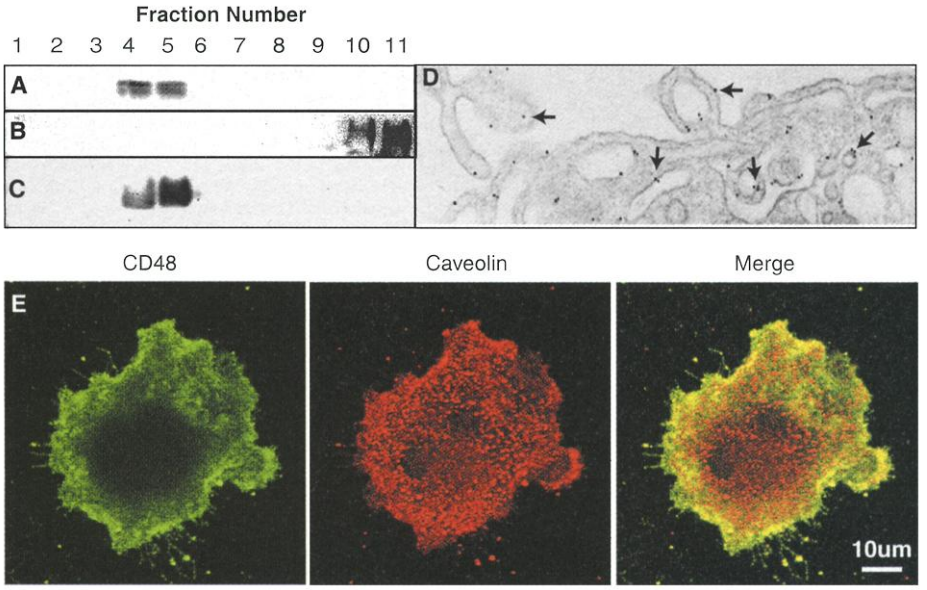

Fig. 1. Localization of caveolae and CD48 in BMMCs. (**A** through **C**) Fractionation of BMMC lysates by means of sucrose gradient centrifugation (*16, 27*). BMMC lysates were subjected to sucrose gradient fractionation, and a portion of each fraction was subjected to SDS–polyacrylamide gel electrophoresis (SDS-PAGE) and immunoblotting with a rabbit caveolin 1–specific antibody (Transduction Labs) (A), mouse clathrin heavy chain–specific antibody (Transduction Labs) (B), and rat CD48-specific antibody (Serotec) (C). The caveolin- and CD48-enriched membrane complexes appeared in the light-density fractions (4 and 5) that corresponded to a white flocculent band in the 15 to 25% sucrose interface. These fractions exclude >95% of cellular proteins. Clathrin heavy chains, which are associated with clathrin-coated pits, were found in distinct fractions (10 and 11). (**D**) Localization of caveolae in BMMCs. Gold particles representing caveolin were specifically localized to the microvilli and to intracellular vesicles (arrows). (**E**) Confocal micrographs of a single plane (0.5 μm thick) showing colocalization of CD48 with caveolin primarily in the plasmalemmal regions of BMMCs. Antibody labels: CD48 (green), caveolin (red), and colocalization (yellow) (*28*).

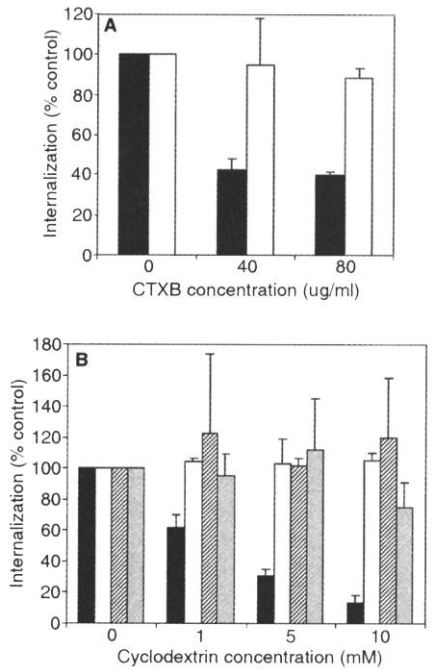

Fig. 2. Specific inhibition of the entry of FimH-expressing bacteria into BMMCs by a caveolae-usurping agent, methyl-β-CTXB (**A**), and a caveolae-disrupting agent, cyclodextrin (**B**). In (A), BMMCs grown on a 96-well plate or cover slips were pretreated with increasing concentrations of CTXB (0 to 80 μg/ml) for 20 min. Either *E. coli* ORN103(pSH2), expressing type 1 fimbriae (*29*) at a MOI of 100, or fluorescent latex beads (0.75 μm in diameter, Polysciences) at a MOI of 300 were added. After incubation for 20 min at 37°C, the cells were assayed (*14, 30*) for uptake of bacteria (black bars) or latex beads (white bars). In (B), BMMCs grown on a 96-well plate were pretreated with increasing concentrations of cyclodextrin (0 to 10 mM) for 10 min in the presence of 10 μM lovastatin. The entry of FimH-expressing *E. coli* (black bars) and latex beads (open bars) was examined as described above. As additional controls, the entry of opsonized FimH$^-$ *E. coli* (hatched bars) and unopsonized FimH$^-$ *E. coli* (gray bars) was assayed. The FimH$^-$ *E. coli* used was *E. coli* strain ORN103(pUT2002) which is an isogenic derivative of ORN103(pSH2) (*29*). Opsonization was performed by incubation of FimH$^-$ *E. coli* with mouse anti–*E. coli* antibody (1:200 dilution). The MOI of opsonized FimH$^-$ *E. coli* was 100, whereas the MOI of the unopsonized FimH$^-$ *E. coli* was 1000. All internalization assays were performed in serum-free RPMI-Hepes buffer. The viability of BMMCs and bacteria was not affected by the treatments with either CTXB or cyclodextrin.

membrane (Fig. 1E), whereas caveolin staining in the interior of BMMCs was vesicular.

CD48 represents the mast cell receptor for FimH-expressing bacteria (*19*). Binding to this receptor induces bacterial entry into BMMCs, with limited loss of bacterial viability (*15*). We investigated whether plasmalemmal caveolae of BMMCs, which contain CD48, were involved in the entry of type 1 fimbriated and FimH-expressing *E. coli*. The binding of cholera toxin B (CTXB) to G_{M1}, clustered within cell surface caveolae, triggers caveolae-mediated internalization of these toxin subunits (*20*). Pretreatment of BMMCs with increasing concentrations of CTXB resulted in up to 60% inhibition of FimH-expressing bacterial entry (Fig. 2A), suggesting that the toxin had usurped available plasmalemmal caveolae and impeded subsequent uptake of FimH-expressing bacteria. However, CTXB did not have any effect on the internalization of latex beads by BMMCs (Fig. 2A). Cyclodextrin is a drug that specifically disrupts caveolar structure by eliminating cholesterol from the cell (*21*). In the presence of increasing concentrations of cyclodextrin, entry of FimH-expressing bacteria into BMMCs exhibited a dose-dependent inhibition (Fig. 2B). Cyclodextrin had no effect on the uptake of latex beads or of opsonized or unopsonized FimH$^-$ *E. coli* by BMMCs (Fig. 2B). Thus, the entry of FimH-expressing bacteria into BMMCs appears to involve plasmalemmal caveolae and FimH.

Fluorescence microscopy of BMMCs with caveolin-specific antibody after exposure to bacteria revealed accumulation of caveolin around internalized bacteria, which suggested that bacterial uptake by BMMCs was accompanied by specific recruitment of cellular caveolae (Fig. 3, A and B). To verify this, we probed infected BMMCs with other markers of caveolae. We found similar recruitment patterns with G_{M1} (Fig. 3, C and D) and with cholesterol (Fig. 3, E and F), confirming that caveolae were being specifically mobilized to sites of bacterial entry. Immunoelectron microscopy with caveolin-specific antibody also revealed the accumulation of caveolin around the bacteria (Fig. 3K). No more than one bacterium was found in a single chamber, implying that caveolae-mediated endocytosis was a progressive process involving uptake of individual bacterium, and thus appeared distinct from the mode of entry of salmonella, in which multiple organisms are internalized in a single phagocytic event (*22*). No caveolar markers accumulated around BMMC-internalized latex beads (Fig. 3, H to J).

We further investigated whether some cellular caveolae were diverted to chambers encasing intracellular bacteria. We therefore developed a fractionation technique that allowed us to simultaneously isolate bacterium-containing chambers and cellular caveolae from the same infected BMMC. To detect bacterium-containing fractions, we prelabeled bacteria with fluorescein isothiocyanate (FITC) before exposure to BMMCs. Localization of caveolae in each fraction was achieved with the use of a caveolin-specific antibody as probe. With the modification of a

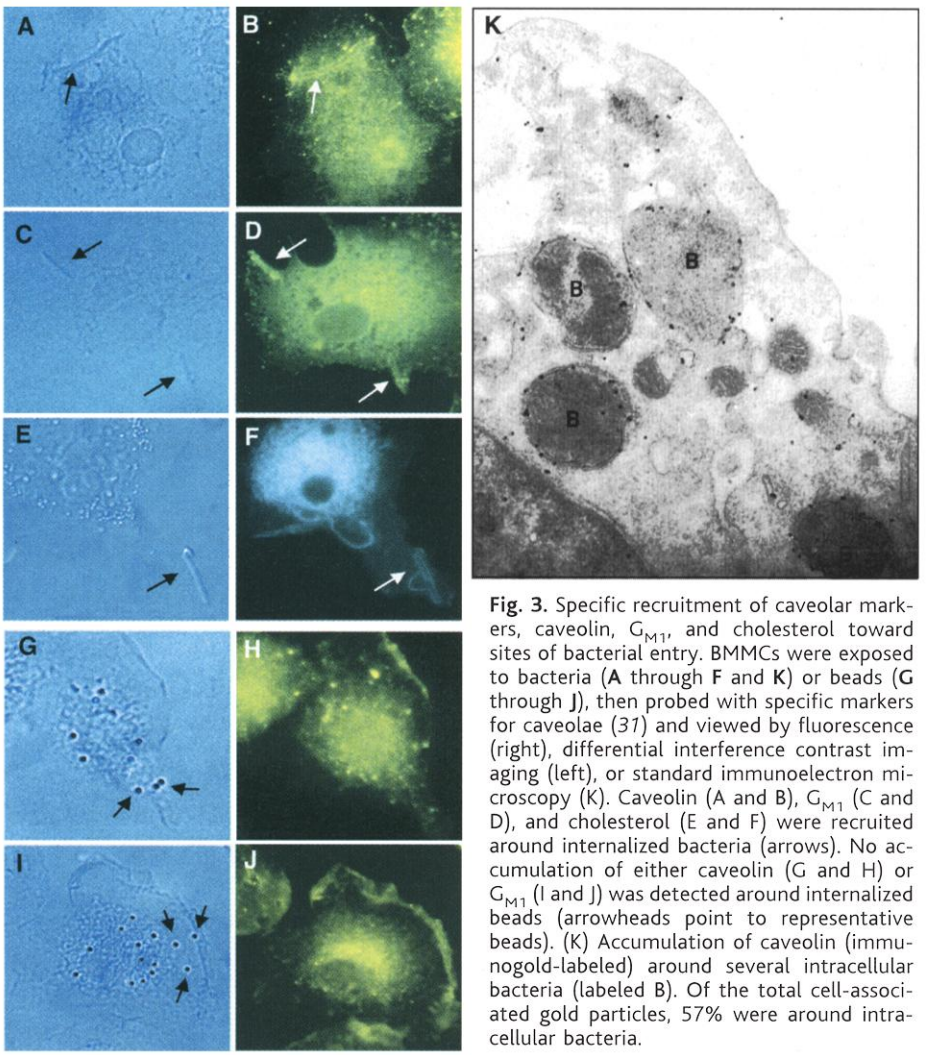

Fig. 3. Specific recruitment of caveolar markers, caveolin, G_{M1}, and cholesterol toward sites of bacterial entry. BMMCs were exposed to bacteria (**A** through **F** and **K**) or beads (**G** through **J**), then probed with specific markers for caveolae (*31*) and viewed by fluorescence (right), differential interference contrast imaging (left), or standard immunoelectron microscopy (K). Caveolin (A and B), G_{M1} (C and D), and cholesterol (E and F) were recruited around internalized bacteria (arrows). No accumulation of either caveolin (G and H) or G_{M1} (I and J) was detected around internalized beads (arrowheads point to representative beads). (K) Accumulation of caveolin (immunogold-labeled) around several intracellular bacteria (labeled B). Of the total cell-associated gold particles, 57% were around intracellular bacteria.

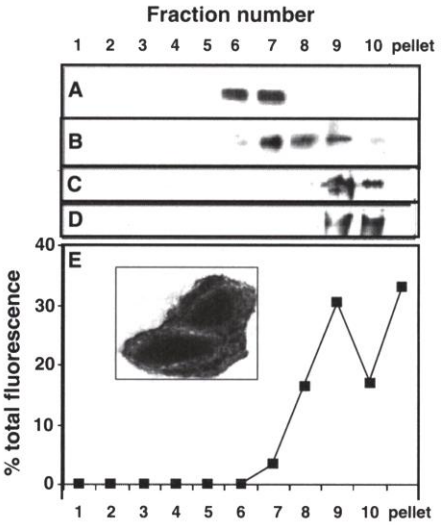

Fig. 4. Cofractionation of caveolar membrane complexes with intracellular bacteria in infected BMMCs. (**A** and **B**) Detection of caveolar fractions from uninfected (A) and infected (B) BMMCs. BMMC homogenates were fractionated over a 5 to 45% discontinuous sucrose gradient (*24*). Eleven fractions, including the pellet, were collected and subjected to SDS-PAGE and immunoblotting with antibody to caveolin. For uninfected BMMCs, a thick white flocculent band was seen at the 25 to 35% sucrose interface corresponding to fractions 6 and 7. For infected BMMCs, the white flocculent band was markedly thinner and a moderately thick yellow flocculent band was present at the 35 to 45% sucrose interface corresponding to fractions 8 to 10. (**C** and **D**) Localization of clathrin heavy chain in fractions from uninfected (C) and infected (D) BMMCs. (**E**) Detection of FITC-labeled bacteria in caveolae-containing fractions. The majority of bacteria were found in fractions 8 to 10, which correspond to where the displaced caveolin and the yellow flocculent band fractionated. The FITC label on the bacteria explains the yellow color of the flocculent band. (Inset) An electron micrograph of a cross section of material isolated from fraction 9.

previously described procedure (*23*, *24*), infected and uninfected (control) BMMCs were homogenized in detergent-free alkaline conditions and were fractionated over a discontinuous sucrose density gradient. Some cellular caveolae shifted from fractions 6 and 7 for uninfected BMMCs (Fig. 4A) to fractions 8 through 10 for infected BMMCs (Fig. 4B). Densitometric analysis of the caveolin bands indicated that fractions 8 to 10 contained 59% of total cellular caveolin. Fluorometric assays of the various fractions from infected BMMCs revealed that the majority of bacteria localized (65%) to fractions 8 through 10, with the peak residing in fraction 9 (Fig. 4E). Electron microscopic examination of thin sections of material in fraction 9 showed the presence of clumps of bacteria-containing vesicles (Fig. 4E, inset). Thus, cellular caveolae appeared to be diverted to form bacteria-encasing compartments. No caveolin was detected in the pellet where the remaining 35% of the bacteria were localized (Fig. 4, B and E). It is presumed that these bacteria were extracellular because free FITC-labeled bacteria, when subjected to fractionation in a parallel assay, localized only to the pellet. The localization of clathrin (fractions 9 and 10) remained the same in uninfected (Fig. 4C) and in infected (Fig. 4D) BMMCs. This indicated a lack of involvement of clathrin in this endocytic process and that the presence of bacteria did not alter the properties of the gradient.

We have shown that bacterial FimH specifically couples to its complementary receptor, CD48, clustered within plasmalemmal caveolae in mast cells. This interaction results in BMMC bacterial uptake mediated by cellular caveolae, which formed distinct intracellular bacterial containment chambers. Because caveolae do not fuse with endosomes (*25*), it is not surprising that *E. coli* contained in caveolar chambers avoid the intrinsic bactericidal activity of BMMCs and remain viable. Although the toxin subunit of *Vibrio cholerae* and FimH-expressing *E. coli* bind distinct receptors on the plasma membrane and are of markedly different sizes, entry of both into BMMCs is mediated by caveolae. These observations reveal convergence among different bacterial species in their capacity to coopt cellular trafficking pathways of the host. They also illustrate the remarkable versatility of caveolae as mediators of a broad range of endocytic processes.

References and Notes

1. E. Yamada, *J. Biophys. Biochem. Cytol.* **1**, 445 (1955).
2. R. G. Anderson, *Annu. Rev. Biochem.* **67**, 199 (1998).
3. R. G. Parton, *Curr. Opin. Cell Biol.* **8**, 542 (1996).
4. P. L. Michael *et al.*, *Mol. Membr. Biol.* **12**, 121 (1995).
5. J. E. Schnitzer, P. Oh, E. Pinney, J. Allard, *J. Cell Biol.* **127**, 1217 (1994).
6. R. G. Anderson, B. A. Kamen, K. G. Rothberg, S. W. Lacey, *Science* **255**, 410 (1992).
7. O. Takashi, A. Schlegel, P. E. Scherer, M. P. Lisanti, *J. Biol. Chem.* **273**, 5419 (1998).
8. A. Schlegel *et al.*, *Cell Signal.* **10**, 457 (1998).
9. A. M. Fra, E. Williamson, K. Simons, R. G. Parton, *J. Biol. Chem.* **269**, 30745 (1994).
10. K. A. Field, D. Holowka, B. Baird, *Proc. Natl. Acad. Sci. U.S.A.* **92**, 9201 (1995).
11. B. Echtenacher, D. N. Mannel, L. Hultner, *Nature* **381**, 75 (1996).
12. R. Malaviya, T. Ikeda, E. Ross, S. N. Abraham, *Nature* **381**, 77 (1996).

13. M. Arock *et al.*, *Infect. Immun.* **66**, 6030 (1998).
14. D. M. Baorto *et al.*, *Nature* **389**, 636 (1997).
15. Z. Gao, J.-S. Shin, R. Malaviya, S. N. Abraham, in preparation
16. E. J. Smart, Y. Ying, C. Mineo, R. G. W. Anderson, *Proc. Natl. Acad. Sci. U.S.A.* **92**, 10104 (1995).
17. W. J. Chang *et al.*, *J. Cell Biol.* **126**, 127 (1994).
18. S. Mayor, K. G. Rothberg, F. R. Maxfield, *Science* **264**, 1948 (1994).
19. R. Malaviya, Z. Gao, K. Thankavel, P. A. Merwe, S. N. Abraham, *Proc. Natl. Acad. Sci. U.S.A.* **96**, 8110 (1999).
20. R. Montesano, J. Roth, A. Robert, L. Orci, *Nature* **296**, 651 (1982).
21. P. G. Yancey *et al.*, *J. Biol. Chem.* **271**, 16026 (1996).
22. J. A. Swanson and S. C. Baer, *Trends Cell Biol.* **5**, 89 (1995).
23. S. K. Song *et al.*, *J. Biol. Chem.* **271**, 9690 (1996).
24. BMMCs (2×10^7) were uninfected or incubated with 10^{10} FITC-labeled *E. coli* [ORN103(pSH2)] for 1 hour at 37°C. BMMCs were lysed with 20 strokes of a Dounce homogenizer in 500 mM sodium carbonate (pH 11) and a cocktail of protease inhibitors. The lysates were adjusted to 45% sucrose and overlaid over a 35 to 5% sucrose gradient and centrifuged as before.
25. P. A. Conrad, E. J. Smart, Y. S. Ying, R. G. Anderson, G. S. Bloom, *J. Cell Biol.* **131**, 1421 (1995).
26. M. Sargiacomo, M. Sudol, Z. Tang, M. P. Lisanti, *J. Cell Biol.* **122**, 789 (1993).
27. BMMCs (2×10^7) were solubilized in 1% Triton X-100, MBS [Mes-buffered saline; 0.25 M NaCl and 25 mM Mes (pH 6.8)] and a cocktail of protease inhibitors in ice for 1 hour without agitation. The cell lysates were adjusted to 40% sucrose in MBS, overlayed with 2 ml of each of 35, 25, 15, and 5% sucrose in MBS, and centrifuged for 18 hours at 39,000 rpm in a SW41Ti rotor (Beckman Instruments). Eleven equal fractions were collected from the top of the gradient and were assayed for protein content, caveolin, clathrin heavy chain, and CD48.
28. BMMCs grown on glass cover slips were fixed with 4% paraformaldehyde. Nonspecific binding was blocked with 10% normal goat serum, and the cells were treated with rat CD48-antibody (1:4) and FITC-conjugated second antibody (Zymed). Cells were washed with phosphate-buffered saline and fixed with 4% paraformaldehyde. After permeabilization, the cells were blocked with 10% normal goat serum and sequentially incubated with rabbit antibody to caveolin (1:100) and TRITC-conjugated second antibody (Zymed). Cover slips were mounted on glass slides and examined with a confocal microscope.
29. S. N. Abraham, D. Sun, J. B. Dale, E. H. Beachey, *Nature* **336**, 682 (1988).
30. After incubation with fluorescent latex beads for 20 min, the BMMC cover slips were exposed to 0.25% trypsin and 0.1 mM EDTA in HBSS (Hanks' balanced salt solution, Gibco-BRL) for 10 min at 37°C and then washed to remove cell surface–bound beads. The number of intracellular beads per 1000 cells was counted by fluorescent microscopy.
31. BMMCs grown on glass cover slips were exposed to *E. coli* [ORN103(pSH2) multiplicity of infection (MOI) = 100] or to latex beads (0.8 μm in diameter, Polysciences, MOI = 300) for 1 hour, repeatedly washed with 10 mM methyl α-D-mannopyranoside to remove surface bound bacteria or beads, and then fixed with 4% paraformaldehyde. Nonspecific binding was blocked with 10% normal goat serum. Caveolin was detected with rabbit antibody to caveolin (1:100) and FITC-conjugated second antibody (1:50); G_{M1} with biotin-labeled CTXB (20 μg/ml, Sigma) and FITC-conjugated streptavidin (1:50, Zymed); and cholesterol with filipin (200 μg/ml). The BMMCs were examined under a fluorescent microscope.
32. We thank S. Ward for electron microscopy and M. Keuhn, L. Hale, and D. Patel for critical review of the manuscript. Supported by NIH grants AI 35678, DK 50814, and CA 14236.

4 April 2000; accepted 16 May 2000